JMEPEG (2012) 21:2188–2194
DOI: 10.1007/s11665-012-0148-9

1059-9495/$19.00

Preliminary Evaluation of the Thermally Affected Metallurgical Condition of Extruded and Drawn CuFe2P Tubes

George Pantazopoulos, Anagnostis Toulfatzis, Sylvia Zormalia, Athanasios Vazdirvanidis, and Dionysios Skarmoutsos

(Submitted February 24, 2011; in revised form January 10, 2012)

The influence of heat treatment conditions on the mechanical behavior and microstructure of CuFe2P (ASTM C19400) in comparison to deoxidized-high-phosphorus (DHP-Cu/ASTM C12200) tubes was investigated. The aim of this study was the enhancement of understanding of microstructure/thermal treatment/strength relationships which could be further utilized for the manufacturing of components exhibiting superior performance and reliability for refrigeration and heat exchanger applications. Microstructural examination employing optical metallography and scanning electron microscopy is used for the evaluation of the recrystallization progress and grain growth processes. In addition, tensile testing was conducted to CuFe2P and DHP tubes following the application of heat treatment cycles, in accordance to the EN 10002-1 specifications. Mechanical properties and microstructure evaluation showed that CuFe2P material is fully recrystallized at 740 °C and DHP at 400 °C for 20 min. Recrystallization initiation varies within the range of 640-660 °C for CuFe2P and below 400 °C for DHP tubes. The tensile strength of the CuFe2P tube decreased from 513 to 367 MPa, the hardness was reduced from 144 to 126 HV, while tensile elongation was significantly improved from 3 to 17%. At 640 °C, only isolated recrystallized areas were evident mainly at the Fe-based intermetallic particle/copper matrix interface areas.

Keywords CuFe2P tube, heat treatment, mechanical testing

1. Introduction

Deoxidized-high-phosphorus (DHP) copper is a widely used material in the form of sheets as common roofing component and for boiler fabrication, while as a tube it is extensively used in water distribution systems, plumbing, medical gas transport, heating, and refrigerant applications because of its high thermal conductivity, good heat transfer characteristics, excellent formability, corrosion resistance, and antimicrobial properties (Ref 1, 2). Design and installation deficiencies and/or the presence of aggressive environment, such as improper water chemistry, may compromise tube reliability and lead to premature failures. Characteristic in-service failures of copper tubes comprise pitting corrosion, stress-corrosion cracking, fatigue, and/or corrosion fatigue, erosion-corrosion, and microbiologically influenced corrosion (MIC) (Ref 3–6). Copper tubing is used also as a vital component in refrigeration industry where high pressures are developed in ecological refrigerant gas systems. Therefore, the need of stronger construction material exhibiting higher performance and high thermal transfer efficiency is compulsory. Moreover, world economy and environmental issues drive toward lighter and cheaper constructions using lower wall thickness tubes which are expected to show high robustness and performance in extreme service environment.

As already established, DHP copper tubes, as conventional pipeline construction component, possess tensile strength ranging from 240 to 300 MPa at the half-hard temper metallurgical condition. Alloy systems such as Cu-Cr-P and Cu-Fe-P provide substantial strength improvement without serious sacrifice of electrical and thermal conductivities. Special precipitation hardening Cu-Cr-P alloys are prone to solution and aging treatment through the application of a series of thermomechanical processes, as reported in Ref 7. The influence of solution and aging treatments along with the applied deformation processes on microstructure-properties relationships in precipitation hardening Cu-0.55wt.%Cr-0.07%P alloy system is presented in Ref 7. Apart from Cr, minor additions of iron (Fe) in Cu-P alloys may raise substantially the tensile strength, through second-phase dispersion, by more than 50% of that exhibited by the conventional DHP-tube component, providing the opportunity for reduction in the respective wall thickness and decrease of weight in the entire pipeline accompanied by subsequent material cost reduction. Such assembly designs are consistent with sustainable development by improving weight, cost, and energy efficiency and effectiveness of the entire heat transfer system.

Strips fabricated by Cu-Fe-P are mainly used as lead frames and other components in electrical/electronic industry. Thorough investigation concerning the effect of thermomechanical process (heat treatment and rolling) on microstructure as well as material hardness, and electrical conductivity of CuFe2P material toward the optimization of industrial applications

George Pantazopoulos, Anagnostis Toulfatzis, Sylvia Zormalia, and **Athanasios Vazdirvanidis**, ELKEME Hellenic Research Centre for Metals S.A., 252 Pireaus Str., 17778 Athens, Greece; and **Dionysios Skarmoutsos**, Halcor S.A. Metal Works, 57th km Athens-Lamia National Highway, 32011 Oinofyta, Greece. Contact e-mail: gpantaz@halcor.vionet.gr.

was studied in Ref 8. Extensive transmission electron microscopy (TEM) studies on the substructure and kinetics of iron phases coarsening and the effect on the electrical properties are reported in Ref 8, 9. The influence of microstructure on electrical conductivity of Cu-Fe-P system by additions of B and Ce was also investigated (Ref 10). High-strength and high-conductivity alloys could be fabricated by appropriate alloy design, by the addition of trace elements such as B, which acts as recrystallization inhibitor, and through the combination of cold deformation and aging treatments (Ref 10).

In the present study, an attempt was made to outline the mechanical behavior of CuFe2P extruded and drawn tubes (with potential applications to the fabrication of tubing for heat exchanger and refrigeration units), as a function of final thermal treatment temperature to understand the respective softening process tendency and to select the optimum conditions for secondary forming operations. Tensile and hardness testing along with optical microscopy and scanning electron microscopy coupled with energy dispersive x-ray spectroscopy were used as the principal analytic techniques for the present investigation.

2. Materials and Methods

Chemical composition limits of the materials studied in the context of the present research are presented in Table 1. Heat treatment trials on CuFe2P and DHP tubes of 10 mm (outer diameter) × 0.50 mm (wall thickness) × 150 mm (length) were conducted. Figure 1 depicts the thermal cycles applied for the purposes of this study where heat treatment temperature varied in the range of 400-740 °C with increment step of ΔT = 20-35 °C and the holding time at soak of 20 min, using a controllable electrical furnace with air recirculation. Low-magnification inspection of surface and fracture morphologies was performed using a Nikon SMZ 1500 stereomicroscope. Microstructural and morphological characterization was conducted on metallographically prepared cross sections after immersion chemical etching in standard $FeCl_3$ solution for approximately 5 s and at the room temperature. The etching solution consists of approximately 8 g $FeCl_3$, 10 mL HCl (37% w/v), and 90 mL de-ionized water. Metallographic evaluation was performed using a Nikon Epiphot 300 inverted metallurgical microscope, while high magnification observations of the microstructure were conducted on ultrasonically cleaned specimens, employing a FEI XL40 SFEG Scanning Electron Microscope and using secondary electron and back-scattered imaging modes for topographic and compositional evaluations. Energy dispersive x-ray spectroscopy, using EDAX system, was also carried out on gold-plated samples for inclusion identification and local elemental chemical analysis. Tensile testing was performed in triplicate samples for each heat treatment condition, according to EN 10002-1 standard using an Instron 5567 electromechanical testing machine with a 30-kN load cell. Tensile elongation measurements were carried out using 50-mm gauge length (referred as A_{50}). Hardness testing was conducted using Instron-Wolpert Vickers microindentation device under 0.2-kg applied load, according to BS EN ISO 6507-1 standard.

3. Results and Discussion

3.1 Microstructure

Optical and SEM micrographs showing the microstructure of CuFe2P tube at the cold worked and at various annealed metallurgical conditions are illustrated in Fig. 2, 3, and 4. As drawn samples' microstructure consists of highly elongated grains toward drawing direction for both CuFe2P and DHP tubes in the as-received (cold-drawn) condition (Fig. 2a and 5a).

Table 1 Chemical composition limits (wt.%) for CuFe2P (C19400) and DHP-Cu (C12200)

Alloy/element	Cu	Fe	Zn	Pb	P
C19400 (CuFe2P)	97.0 min	2.1-2.6	0.05-0.20	0.03 max	0.015-0.15
C12200 (DHP-Cu)	99.90 min	...	...	...	0.015-0.040

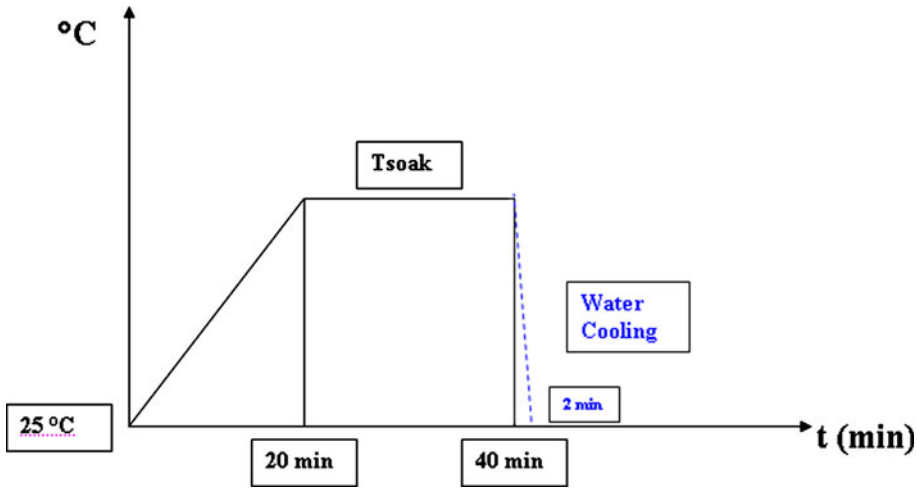

Fig. 1 Schematic drawing of the annealing cycle for CuFe2P and DHP tubes. Heat treatment parameters [temperature (*T*) and time (*t*)]

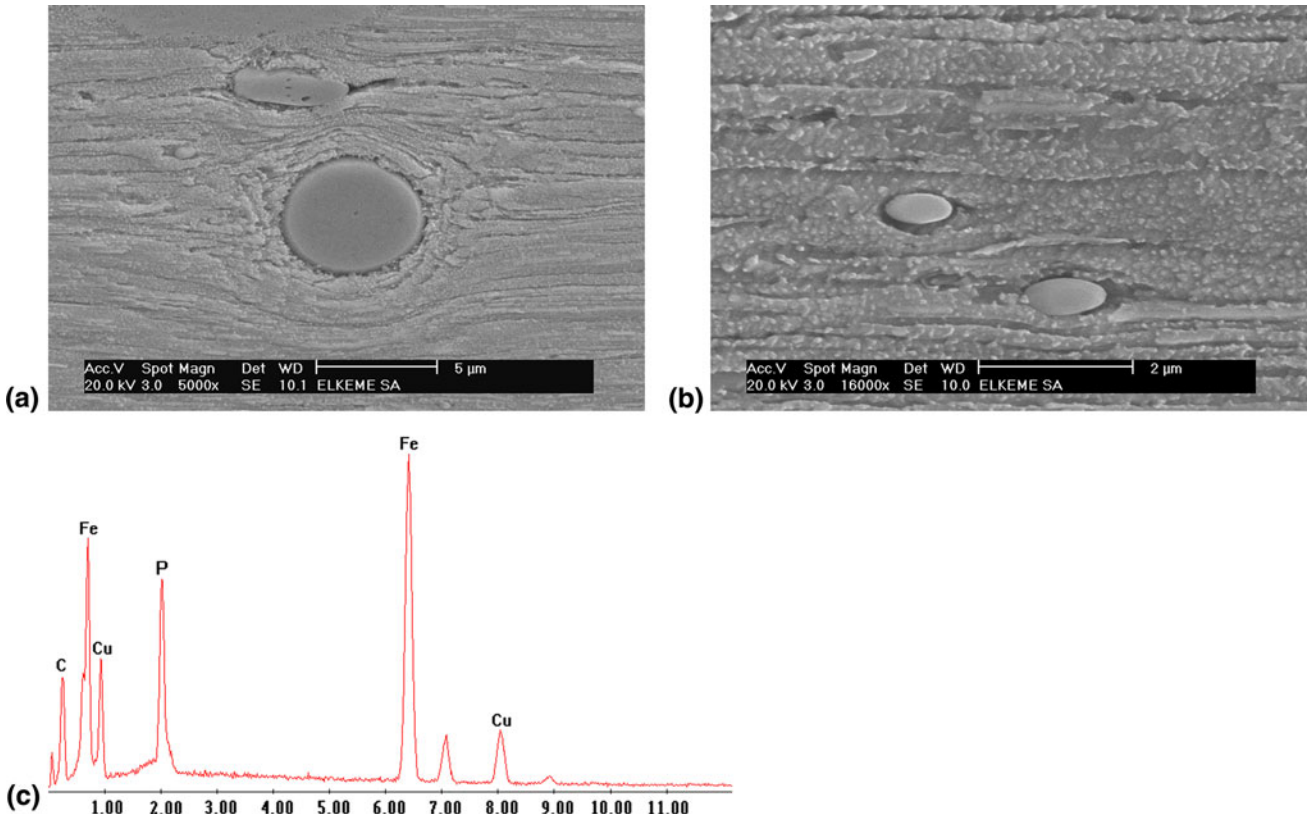

Fig. 2 SEM micrographs showing (a) the flow lines around the Fe-based particles and the elongated grain structure, (b) fine dispersoids homogeneously distributed in the matrix and oval-shaped Fe-based particles of sample at the as-received condition (c) representative EDS spectrum of Fe-based particle (longitudinal section)

The initiation of CuFe2P recrystallization at 640 °C is verified by new grains nucleation at the vicinity of Fe-particles/matrix interface (Fig. 3). Isolated equiaxed recrystallized grains dispersed in an elongated matrix started to appear at that heat treatment temper (640 °C), as shown in Fig. 3(b). Mixed grain structure is observed at 720 °C with a shell of recrystallized grains near the outer tube surface and cold-drawn structure near the inner surface (Fig. 4a). The reason for the existence of such ''sandwich''-type structure, of recrystallized grain and cold-worked layers, should be further investigated. Potential root cause(s) of the above mentioned heterogeneity might be the differential strain energy and/or non-uniform iron particle distribution.

Iron-containing intermetallic particles exhibited a pronounced variation in size, from ≤ 1 µm reaching up to $\sim$10 µm, and shape complexity (irregularity). The particles' morphology varied from coarse spheroid and angular plate-like up to fine sub-microscopic dispersoids uniformly distributed in the copper matrix (Fig. 2b and 3a), while their chemical composition is approximately equivalent, as determined by EDS analysis. Iron is slightly dissolved in Cu matrix, forming a solid solution with max. solubility up to almost 1.1% at 850 °C, without forming any intermediate intermetallic compound, as dictated by the binary Cu-Fe equilibrium phase diagram (Ref 1). However, mixed ternary intermetallics consisting of Fe-Cu-P may be formed; this issue could be addressed through a different perspective by thermodynamic modelling and x-ray diffraction, which is out of the context of the present investigation. A characteristic EDS spectrum of a round iron-rich particle is shown in Fig. 2(c). Submicroscopic (<1 µm) dispersoids tend to be strong grain boundaries pinners, retarding recrystallization and grain boundary migration. Moreover, irregular- and angular-shaped particles may serve as stress raisers (notch-effect) and could lead to premature failures during service. It was concluded that the size and distribution of Fe-rich dispersoids play a vital role in recrystallization kinetics. Strain localization induced by the non-uniform plastic flow at the particle/matrix interface affects the local nucleation rate and hence, the recrystallized grain size. An example of early subgrain formation at the particle/matrix interface driven by localized strain gradient is presented in Fig. 3(a).

CuFe2P material displays a non-uniform and non-equiaxed grain structure (pancake structure), developed in a very narrow temperature range (mostly within 720-740 °C, while full recrystallization was observed after 740 °C heat treatment) with respect to the entire temperature range used, where a reliable quantitative relationship between grain size and strength cannot be achieved.

Fully recrystallized CuFe2P grain structure was achieved at 740 °C (Fig. 4b), while DHP-Cu was fully recrystallized at much lower temperature of 400 °C, with average grain size $\sim$10 µm (Fig. 5b). The evolution of microstructure of DHP-Cu tube as a function of heat treatment temperature is presented in Fig. 5. Fibered and strongly deformed microstructure to twinned equiaxed grain structure of grain size from 10 to over 100 µm is shown in the respective micrographs representing the main stages of recrystallization and grain growth in the common DHP alloy system studied for comparison purposes. The grain size of DHP observed at 740 °C is 100 µm due to

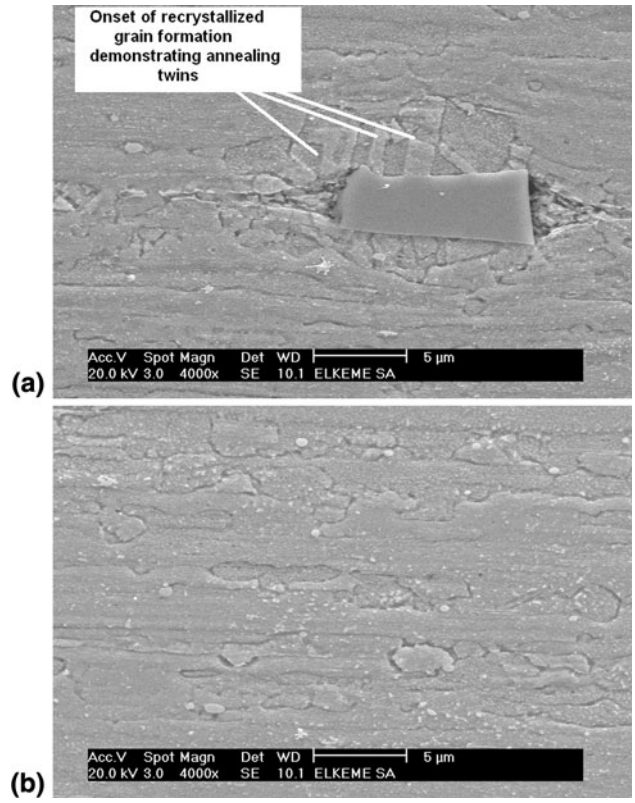

Fig. 3 SEM micrographs showing (a) the recrystallized grains at the vicinity of the Fe-based intermetallic particle/matrix interface (longitudinal section). The formation of recrystallized twinned grains at the matrix/particle interface and (b) the partially recrystallized grain structure of sample heat treated at 640 °C

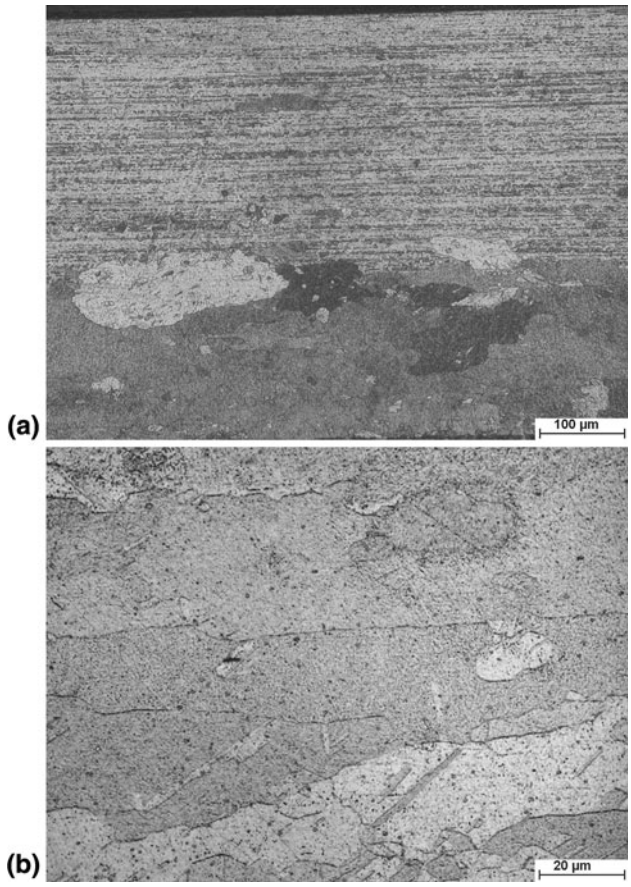

Fig. 4 Optical micrographs showing the CuFe2P alloy grain structure, which consists of (a) partially recrystallized grains in sample heat treated at 720 °C and (b) fully recrystallized "pancake-type" grains in sample heat treated at 740 °C (longitudinal section). Note the occasionally found annealing twins. Dark "dots" correspond to Fe-rich particles

enhanced grain coarsening (Fig. 5d). CuFe2P alloy-recrystallized grain structure consists of non-uniform and "pancake"-type grains with sporadically found thermal twins (Fig. 4b), while DHP consists of equiaxed grain structure with multiple annealing twins, which may be considered as a typical microstructure of conventional high-purity copper (Fig. 5b-d).

3.2 Mechanical Properties

The variation of tensile properties as a function of soaking temperature is shown in Fig. 6(a)-(c) for both CuFe2P and DHP-Cu materials. Tensile, proof strength, and average hardness decreased as the soaking temperature increased (see Table 2; Fig. 6a and 7a). As-drawn CuFe2P tubes (hard condition) exhibited tensile strength up to 513 MPa, 0.2% offset yield strength (also referred as proof strength) of 477 MPa, and almost null fracture elongation (3%). Heat treatment caused a decreasing tendency in tensile strength from 443 to 302 MPa and in 0.2% offset yield strength from 384 to 118 MPa, while fracture elongation showed an incremental tendency from 14 to 31% (Fig. 6c). However, there is almost a "plateau" indicating relatively limited hardness sensitivity on temperature change between 450 and 610 °C, as anticipated also by the softening rate shown in tensile strength as a function of soaking temperature (Fig. 7a). Softening rate increased significantly above a temperature threshold between 640 and 660 °C which could be also justified by the initiation and progress of recrystallization. Hardness also decreased with a higher rate above 640 °C (Fig. 7a). These findings, concerning hardness and strength changes, may be attributed to the advancement of recrystallization and grain growth processes.

The tensile elongation of CuFe2P tube increases continuously for heat treatment temperatures above 660 °C, which is consistent with recrystallization-induced softening phenomena, while, in case of DHP, tube elongation reaches a maximum value at 425 °C temperature and then drops as a result of grain coarsening (Fig. 6c). As-drawn DHP tubes (hard condition) exhibited tensile strength up to 485 MPa, 0.2% offset yield strength 477 MPa, and almost null fracture elongation (2%), see Table 3. Tensile strength decreased from 259 to 221 MPa, 0.2% offset yield strength from 81 to 37 MPa for soaking temperatures varied from 400 to 740 °C (Fig. 6b). Fracture elongation reaches a maximum value of 40% for 425 °C soaking temperature and then drops continuously to 22% for 740 °C soaking temperature (see Fig. 6c; Table 3). The interpretation of the drop of fracture elongation is attributed to grain-coarsening processes occurred above a certain temperature threshold (425 °C). Moreover, hardness values are consistent for DHP soft annealed temper (Fig. 7b). Softening curves plotted for DHP-Cu demonstrate

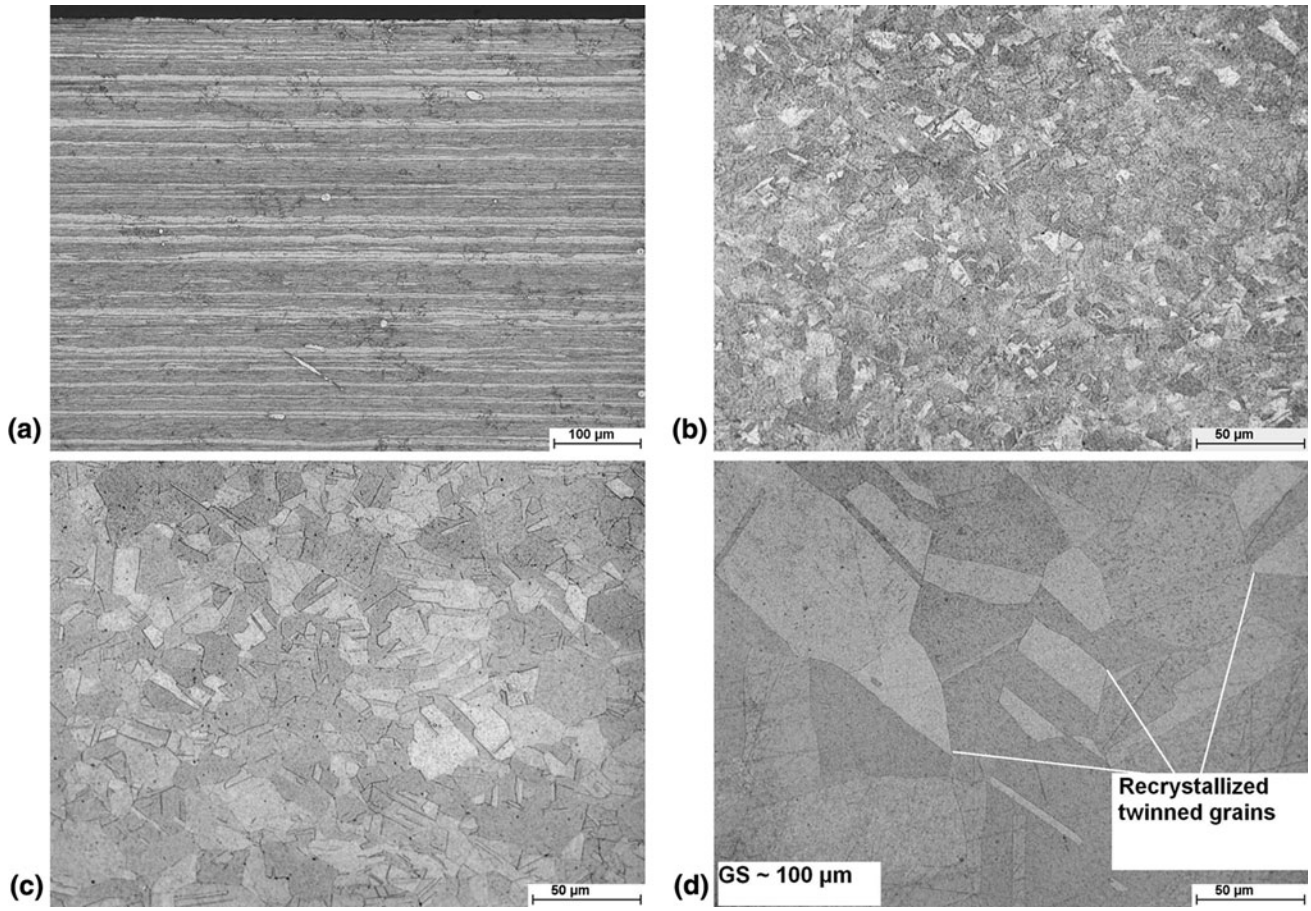

Fig. 5 Optical micrographs showing the DHP grain structure, which consists of (a) cold-worked fibered grains, (b) fully recrystallized grains in sample heat treated at 400 °C with grain size ~10 µm, (c) sample heat treated at 550 °C with grain size up to ~22 µm, (d) sample heat treated at 740 °C with grain size up to 100 µm (longitudinal section)

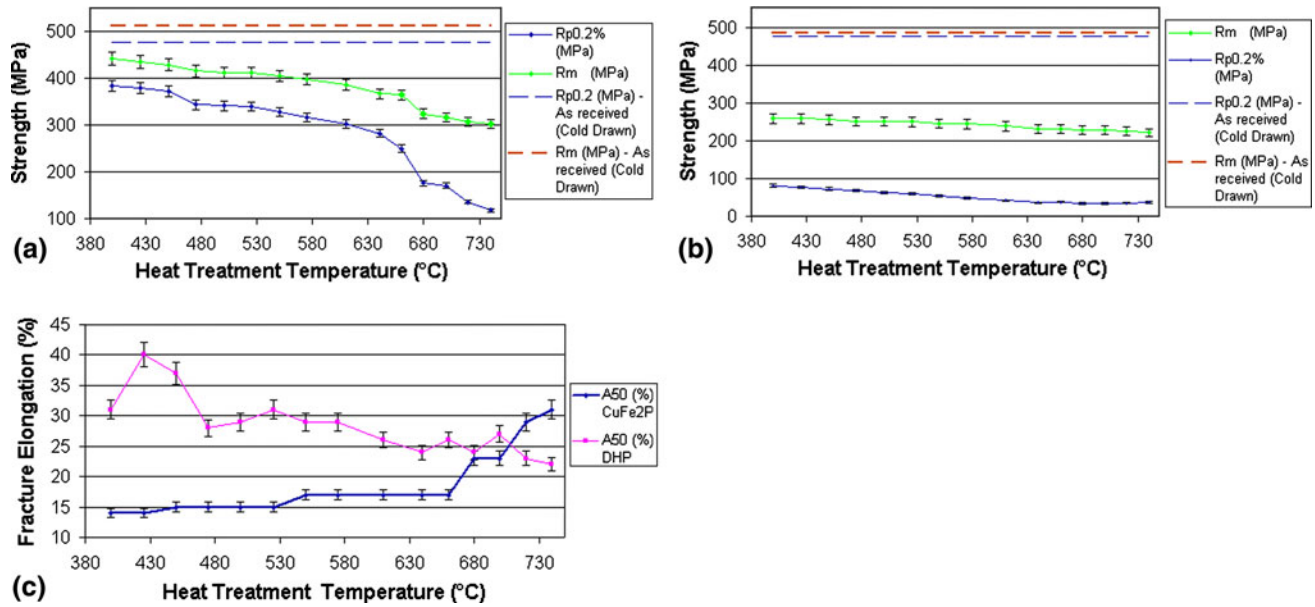

Fig. 6 Diagrams showing variation of 0.2% yield and tensile strength (a) for CuFe2P, (b) DHP-Cu, and (c) fracture elongation for both CuFe2P and DHP as a function of heat treatment temperature. Mean values of tensile properties were plotted using the average of three independent measurements, while error bars were estimated approximately using the induced relevant standard deviation

Table 2 Mechanical properties as a function of heat treatment temperatures (CuFe2P)

Sample ID	Heat treatment temperature, °C	Wall thickness, mm	Diameter, mm	$Rp_{0.2}$, MPa	Rm, MPa	A_{50}, %	$HV_{0.2}$
1	As-received-hard drawn	0.50	10.0	477	513	3	144
2	400	0.50	10.0	384	443	14	143
3	425	0.50	10.0	380	436	14	141
4	450	0.50	10.0	373	429	15	133
5	475	0.50	10.0	344	416	15	133
6	500	0.50	10.0	342	412	15	134
7	525	0.50	10.0	340	412	15	131
8	550	0.50	10.0	328	406	17	134
9	575	0.50	10.0	316	399	17	135
10	610	0.50	10.0	302	386	17	131
11	640	0.50	10.0	283	367	17	126
12	660	0.50	10.0	250	365	17	...
13	680	0.50	10.0	176	325	23	107
14	700	0.50	10.0	171	317	23	93
15	720	0.50	10.0	136	308	29	87
16	740	0.50	10.0	118	302	31	74

$Rp_{0.2}$ 0.2% offset yield strength, Rm ultimate tensile strength A_{50} tensile elongation measured at 50-mm gauge length, $HV_{0.2}$ Vickers hardness under 0.2-kg force applied load

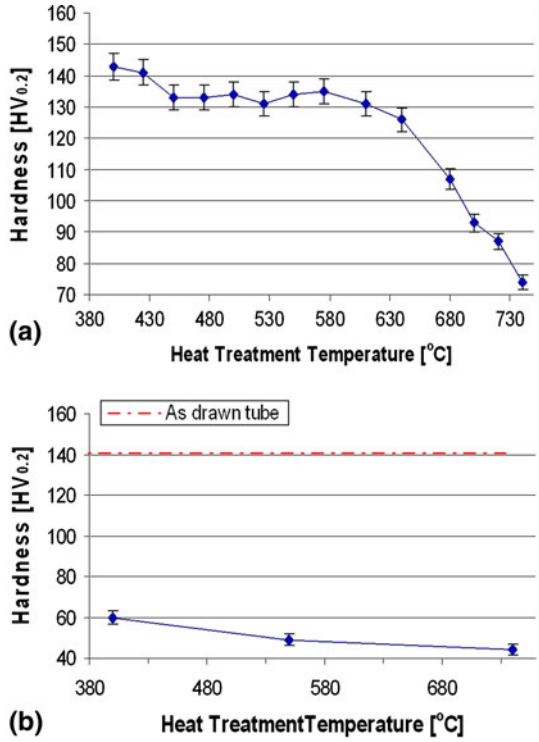

Fig. 7 Hardness variation as a function of heat treatment temperature for (a) CuFe2P alloy and (b) DHP-Cu. Mean values of hardness were plotted using the average of three independent measurements, while error bars were estimated approximately using the induced relevant standard deviation

much lower slopes, as compared to those presented for CuFe2P (see Fig. 6a and b), since DHP has been already fully recrystallized and stabilized at 400 °C. DHP exhibited generally higher softening at 400 °C, showing also much lower values in tensile strength, as compared with CuFe2P, at the respective heat treatment conditions, in a percentage varying from 27% (heat treatment condition: 740 °C/20 min) to 42% (heat treatment condition: 400 °C/20 min).

4. Conclusions and Perspectives for Future Research

The influence of heat treatment on mechanical behavior of 10×0.5 mm CuFe2P (C 19400) tubes was investigated compared with the conventional DHP (C 12200) tubes for industrial heat exchanger applications. CuFe2P material exhibited much higher softening resistance up to 400 °C, since submicroscopic iron precipitates constitute inherent obstacles for recrystallization and grain boundary migration. More specifically, the present investigation results may lead to the following conclusions:

(1) CuFe2P tube is fully recovered, possessing only localized recrystallized areas for temperature up to ~640 °C. Tensile strength dropped from 513 to 367 MPa, hardness was reduced from 144 to 126 HV, and tensile elongation increased significantly from 3 to 17%. At 640 °C, only isolated recrystallized areas are evident mainly at the Fe-based intermetallic particle/copper matrix interface areas.

(2) Between 660 and 720 °C, the material is partially recrystallized with recrystallized grains near the outer tube surface, while full recrystallization was achieved at 740 °C. CuFe2P sample at that temper consists of non-uniform and pancake-type grains with rarely found thermal twins. Final tensile strength was 302 MPa, fracture elongation was 31%, and hardness was 74 HV.

(3) DHP copper is fully recrystallized at 400 °C. Grain growth occurred between 425 and 740 °C, leading to a coarse grain size of ~100 μm. A sharp drop in strength, e.g., tensile strength from 477 to 259 MPa, and hardness from 141 to 60 HV—consistent with soft annealed

Table 3 Mechanical properties as a function of heat treatment temperatures (DHP)

Sample ID	T heat treatment for 20 min, °C	Wall thickness, mm	Diameter, mm	$Rp_{0.2}$, MPa	Rm, MPa	A_{50}, %	$HV_{0.2}$
1	As-received-hard drawn	0.50	10.0	477	485	2	141
2	400	0.50	10.0	81	259	31	60
3	425	0.50	10.0	77	258	40	···
4	450	0.50	10.0	72	256	37	···
5	475	0.50	10.0	68	251	28	···
6	500	0.50	10.0	63	251	29	···
7	525	0.50	10.0	60	250	31	···
8	550	0.50	10.0	53	245	29	49
9	575	0.50	10.0	48	244	29	···
10	610	0.50	10.0	42	238	26	···
11	640	0.50	10.0	36	231	24	···
12	660	0.50	10.0	38	230	26	···
13	680	0.50	10.0	34	227	24	···
14	700	0.50	10.0	34	229	27	···
15	720	0.50	10.0	35	224	23	···
16	740	0.50	10.0	37	221	22	44

$Rp_{0.2}$ 0.2% offset yield strength, Rm ultimate tensile strength, A_{50} tensile elongation measured at 50 mm gauge length, $HV_{0.2}$ Vickers hardness under 0.2 kg force applied load

temper, occurred at 400 °C—in contrast with CuFe2P alloy, which exhibited a gradual reduction in strength, but with higher softening rate for $T > 640$ °C. Recrystallized grain structure of DHP copper consists of equiaxed grains with multiple annealing twins. DHP softening curve almost flattened out over soaking temperature up to 550 °C.

(4) The above findings suggest strongly that CuFe2P alloy stands as an important candidate material, since it combines high strength (Rm > 300 MPa) and sufficient ductility (up to ~30%) as compared with conventional DHP copper, providing also significant benefit for design modifications aiming to lower the weight of the installations and augment reliability and cost improvement. In addition, service life extension due to increase of erosion and wear damage tolerance of the pipeline made of CuFe2P is also expected.

The current results constitute the preliminary findings aiming to acquire deeper knowledge toward the manufacture and cost of high reliability components, maintaining also the superior physical properties of high-purity copper, in combination with improved energy efficiency. Higher resolution and nano-scale microstructural investigation could be suggested for the study of substructure evolution and the influence of iron-based submiscroscopic particles on dislocation dynamics and grain boundary migration. Furthermore, corrosion and thermal conductivity assessments, as a function of temper (metallurgical condition), could be planned as a future step of the research study to evaluate the performance of the entire heat transfer unit under industrial service conditions.

Acknowledgments

The authors wish to express special thanks to Dr. G. Tsinopoulos for the constructive technical discussion, and Mr. A. Rikos for his valuable contribution to the experimental study.

References

1. ASM Specialty Handbook, *Copper and Copper Alloys*, 1st printing, ASM International, Materials Park, 2001
2. G. Joseph, *Copper: Its Trade, Manufacture, Use and Environmental Status*, 2nd printing, ASM International, Materials Park, 2001
3. G. Pantazopoulos, A. Vazdirvanidis, and G. Tsinopoulos, Failure Analysis of a Hard Drawn Water Tube Leakage Caused by the Synergistic Actions of Pitting Corrosion and Stress-Corrosion Cracking, *Eng. Fail. Anal.*, 2011, **18**, p 649–657
4. M.E. Stevenson, M.E. Barkey, and J.L. McDougall, Stresses in Bent Copper Tubing. Application to Fatigue and Stress-Corrosion Cracking Failure Mechanisms, *J. Fail. Anal. Prev.*, 2005, **5**(6), p 25–29
5. B. Kuznicka, Erosion-Corrosion of Heat Exchanger Tubes, *Eng. Fail. Anal.*, 2009, **16**(7), p 2382–2387
6. A.M. Olszewski, Avoidable MIC-Related Failures, *J. Fail. Anal. Prev.*, 2007, **7**(4), p 238–246
7. H. Gao, T. Tiainen, E. Huttunen-Saarivita, and Y. Ji, Influence of Thermomechanical Processing on the Microstructure and Properties of a Cu-Cr-P Alloy, *J. Mater. Eng. Perform.*, 2002, **11**(4), p 376–383
8. Z.M. Rdzawski, J. Stobrawa, and W. Głuchowski, Structure and Properties of CuFe2 Alloy, *J. Achiev. Mater. Manuf. Eng.*, 2009, **33**(1), p 7–18
9. R. Monzen, T. Tada, T. Seo, and K. Higashimine, Ostwald Ripening of Rod-Shaped α-Fe Particles in a Cu Matrix, *Mater. Lett.*, 2004, **58**(14), p 2007–2011
10. D.-P. Lu, J. Wang, W.-J. Zeng, Y. Liu, L. Lu, and B.-D. Sun, Study on High-Strength and High-Conductivity Cu-Fe-P Alloys, *Mater. Sci. Eng. A*, 2006, **421**, p 254–259